Grid Surveillance and Diagnostics using Power Line Communications

Yinjia Huo, Gautham Prasad, Lazar Atanackovic, Lutz Lampe, and Victor C. M. Leung

Department of Electrical and Computer Engineering, The University of British Columbia

Email: {yortka, gauthamp}@ece.ubc.ca, lazar_a@shaw.ca, {lampe, vleung}@ece.ubc.ca

Abstract—With an aging power distribution infrastructure, it becomes increasingly important for the next generation smart grid to self-monitor its transmission lines. In this paper, we propose a road-map towards achieving a self-reliant grid surveillance using power line communications (PLC). To this end, we exploit the principle that cable faults or degradations manifest themselves as changes in the PLC channel conditions. In particular, by monitoring the channel transfer functions that are already computed in legacy PLC receivers, we enable power line modems with intelligent grid sensing abilities to identify and assess cable anomalies using machine learning techniques. Through simulations, we show that our proposed monitoring and diagnostics solutions successfully empower power line modems to independently detect and predict the extent of water-tree degradations commonly seen in cross-linked polyethylene insulated power cables.

I. INTRODUCTION

A smart-grid (SG) equips utility companies with complete visibility and pervasive control over their assets and services [1]. To this end, a consistent monitoring of the power cable status is of crucial importance as a large part of the power distribution system infrastructure is aging and suffering from considerable underinvestment [2, Ch. 2]. An ever increasing demand and congestion level is also making it increasingly difficult to schedule circuit outages for routine maintenance and upgrades [2, Ch. 2]. As a result, a non-destructive on-line monitoring of the wiring infrastructure is desirable to utility companies so that preemptive measures can be taken to avoid a possible in-service failure in the grid [3, Ch. 6].

Several online monitoring and diagnostics methods have been developed and applied in the past, such as, bulk property diagnostics based on dissipation factor measurements [4], as well as localized degradation diagnostics based on reflectometry or partial discharge tests [5], [6]. However, these methods do not possess the ability to self-diagnose, i.e., the results demand manual interpretation, and require the use of external devices or additional sensors, which introduces extra costs [3, Ch. 6]. Therefore, a self-sustainable infrastructure that can constantly monitor its health and auto-diagnose faults or degradations is more suitable in the context of SGs.

Considering these requirements, the use of power line communications (PLC) for grid surveillance and diagnosis is an attractive alternative or a supplement to legacy methods.

PLC uses the existing power distribution infrastructure for data communication, and PLC-based communication systems have already been developed for power distribution automation systems [7], [8]. In our work, we further extend its usage by utilizing the deployed power line modems (PLMs) for grid surveillance. The use of PLMs for network sensing have previously been achieved to determine the network topology [9], or detect high- and low-impedance faults [10]. Furthermore, the communication channel estimate, which is commonly computed inside legacy PLMs, has also been used in the past to detect and localize a fault [11], [12]. However, these works are unable to monitor the status of the power line in terms of identifying non-localized homogeneous degradations or estimating the extent of degradation.

In this paper, we exploit the principle that any fault or degradation causes distinctive changes in the broadband power line communication (BB-PLC) channel frequency response (CFR), which can be used not only to detect the presence of a fault or degradation, but also determine the type of degradation, whether localized or homogeneous, and further estimate the extent of the degradation. However, the problem is perplexed by changes in load conditions that also lead to a change in the CFR. To counter this issue, we use machine learning (ML) techniques, analogous to [11], to train a machine with varying degradation situations under different load conditions, so that it is then able to automatically diagnose a degradation anytime in the future. Note that ML-based approaches have also been previously employed in [13], [14] to enable automatic detection of faults by passively monitoring cable voltage and current values.

For our investigation, we consider power lines with cross-linked polyethylene (XLPE) cable insulations that are often subjected to water-tree (WT) degradations [15]. However, our methods can also be applied for diagnosis of alternative types of degradations and faults as well.

Nomenclature: Throughout this paper, we use $\Re(x)$ and $\Im(x)$ to indicate the real and imaginary parts of a complex number x. We denote a uniform random distribution between a and b as $\mathscr{U}(a, b)$.

II. MODELING WATER TREE DEGRADATION

We first describe our WT degradation modeling strategy, including the cable aging profile that we use to emulate a realistic cable degradation.
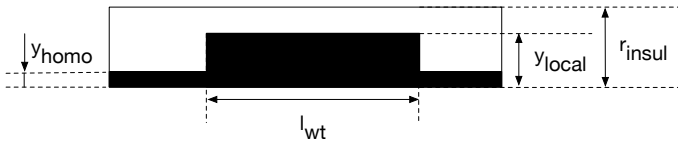
Fig. 1. Aging profile of water tree degradation along a cable.

TABLE I
CABLE PARAMETERS [20]–[22], [23, P. 794]

Dielectric yield strength (Y)	2×10^7 Pa
Size of the free-volume voids (v_0)	2.5×10^{-28} m^3
Diffusion constant of water into the dielectric (n_0)	1.44×10^4
Absolute permittivity (ϵ_0)	8.8×10^{-12} F/m
Relative permittivity of non-degraded XLPE (ϵ_{PE})	$2.3 - 0.001j$
Depolarization factor (D)	$\frac{1}{12}$
Absolute water content in the WT region (q_w)	0.06
Conductivity of water (σ_w)	0.22 S
Mains frequency on the line (f_0)	60 Hz

A. Cable Aging Profile

Widely deployed extruded cables with insulations like XLPE are mainly degraded by electrical aging, i.e., WT and electric treeing (ET) degradation [16]. In this paper, we focus on monitoring WT degradation, which is an important contributing factor to ET inception [17]. It has been shown that many power lines exhibit near-uniform degradation across the length after many years of service [18]. However, spots with intensive water ingress and/or local defects (e.g., protruded semiconductor coating, and voids), are breeding grounds for salient localized WT degradations [19]. Thus, to faithfully emulate a realistic degraded cable, we model the WT degradation to be homogeneous along the cable with a degradation depth y_{homo}, which is a portion of the total insulation thickness r_{insul}. On top of this, we include a possible localized WT degradation with a degradation depth y_{local} ($y_{local} > y_{homo}$) and a length ℓ_{wt}, which may be present anywhere along the cable, as shown in Fig. 1.

B. Effect of WT Degradation

The impact of WT degradation on the dielectric properties of the XLPE insulation has already been investigated in the literature [22], [24]. For the WT degraded region, i.e., the shaded region in Fig. 1, the relative permittivity can be computed as [24]

$$\epsilon_{WT} = \epsilon_{PE}\left(1 + \frac{q_w(\epsilon_w - \epsilon_{PE})}{D(1 - q_w)(\epsilon_w - \epsilon_{PE})}\right), \quad (1)$$

where ϵ_w is the permittivity of water that is given by $\epsilon_w = 81 - j\frac{\sigma_w}{2\pi f \epsilon_0}$, with σ_w being the conductivity of water and f being the frequency of operation. All other parameters of (1) are tabulated in Table I along with the values used. We can then compute the overall permittivity for any degradation depth y of the the total insulation thickness r_{insul} as [22, Eq. 6.3]

$$\epsilon_{total} = \left(\frac{\gamma}{\epsilon_{WT}} + \frac{1 - \gamma}{\epsilon_{PE}}\right)^{-1}, \quad (2)$$

where the degradation severity is defined as $\gamma \triangleq y/r_{insul}$. For the structure shown in Fig. 1, the section of cable with localized WT degradation has $\gamma_{local} = y_{local}/r_{insul}$, while for other sections of that cable, $\gamma_{homo} = y_{homo}/r_{insul}$. Further, the homogeneous WT degradation depth incurred over time t can be computed as [21]

$$y_{homo} = \sqrt[3]{\frac{1}{Y}\left(n_0 v_0 f_0 F^2 \epsilon_0 \Re\{\epsilon_w\}\sqrt{t^3}\right)}, \quad (3)$$

where F is the electric field strength (see Section III-D). The remaining parameters are all listed in Table I along with their values that we use in our model.

III. MODELING BB-PLC CHANNELS

In this section, we describe the BB-PLC channel modeling technique that we use, including the cable characterization in the form of its per-unit-length (PUL) parameters.

A. Channel Modeling Strategy

In order to accurately capture the effects of the insulation dielectric property changes on the channel frequency response with a given aging profile (e.g., Fig. 1), we choose the bottom-up method for channel modeling [25], [26]. Each section along the cable with the same degradation severity can be viewed as a uniform line with electrically small cross-sectional dimensions, where BB-PLC signals are transmitted in a quasi-transverse-electromagnetic (quasi-TEM) propagation mode. Hence, we use the transmission line theory, and in particular, multiconductor transmission line (MTL) theory to account for a general case of power lines with more than two conductors [25]. For each section of a constant degradation severity we model the channel using the MTL equations [27, Chs. 1, 3], and finally concatenate all sections to obtain the overall CFR between any two points of interest.

B. PUL Parameters Computation

CFR computation using MTL equations require the characterization of the cables in the form of their PUL parameters of resistance ($\mathbf{R}$), inductance ($\mathbf{L}$), capacitance ($\mathbf{C}$), and conductance ($\mathbf{G}$) matrices. For power line cables consisting of N conductors ($N \geq 2$), each of the $\mathbf{R}$, $\mathbf{L}$, $\mathbf{C}$, and $\mathbf{G}$ matrices are of dimensions $(N - 1) \times (N - 1)$. By denoting the reference conductor as the 0-th line and PUL resistance for the i-th line as R_i ($0 \leq i \leq (N-1)$), we obtain each of the (i, j)th element of $\mathbf{R}$ as [27, Eq. 3.12]

$$R_{ij} = R_0 + R_j, \quad i = j, \quad (4)$$
$$R_{ij} = R_0, \quad i \neq j. \quad (5)$$

Since the medium surrounding the conductors, in most cases, is non-ferromagnetic with permeability of free space, i.e., $\mu = \mu_0 = 4\pi \times 10^{-7}$ H·m^{-1}, and since permittivity of the surrounding medium is irrelevant in determining $\mathbf{L}$, we deem the surrounding medium to be free space for the computation of $\mathbf{L}$ [27, Ch. 3]. Under such conditions, we apply the wide
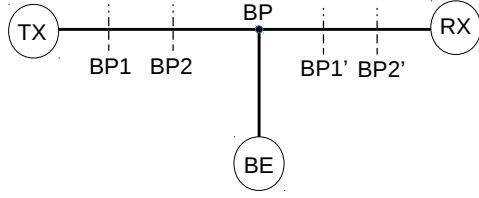
Fig. 2. An example of a PLC network topology, where a localized degradation is present either in the section BP1-BP2 or BP1′-BP2′.

TABLE II
PROPERTIES OF THE N2XSEY THREE-CORE CABLE [31]

Conductance separation (d_{cond})	15.8 mm
Conductance radius (r_{cond})	3.99 mm
Number of strands	19
Strand radius	0.915 mm
Copper conductance	5.96×10^7 S/m
Maximum Rated Voltage (V_0)	12 kV

separation approximations for round conductors to get [27, Eq. 5.23]

$$L_{ij} = \frac{\mu_0}{2\pi} \ln\left(\frac{d_{0,j}^2}{r_0 r_j}\right), \qquad i = j, \qquad (6)$$

$$L_{ij} = \frac{\mu_0}{2\pi} \ln\left(\frac{d_{0,i} d_{0,j}}{r_0 d_{i,j}}\right), \qquad i \neq j, \qquad (7)$$

where r_j is the radius for the j-th conductor and $d_{i,j}$ is the separation distance between the ith and jth conductors.

For a general wire configuration with an inhomogeneous surrounding medium, a numerical solver based on the finite element method is required to solve the Laplace equation to derive the $\mathbf{C}$ and $\mathbf{G}$ matrices [26]. However, we found this to consume enormous amounts of time for PUL calculations for various degradation severities. Therefore, to reduce complexity of PUL computation, we assume a homogeneous surrounding medium with a permittivity of ϵ_{total}. Under such conditions, we can compute the capacitance and conductance matrices as [27, Eq. 5.24]

$$\mathbf{C} = \mu_0 \epsilon_0 \Re(\epsilon_{total}) \mathbf{L}^{-1}, \qquad (8)$$

$$\mathbf{G} = \mu_0 \sigma \mathbf{L}^{-1}, \qquad (9)$$

where σ is the conductance of the insulation, which can be represented in terms of the complex permittivity as [26, Eq. 7], [22]

$$\sigma = -2\pi f \epsilon_0 \Im(\epsilon_{total}). \qquad (10)$$

Using (10) in (9), we get

$$\mathbf{G} = -2\pi f \mu_0 \epsilon_0 \Im(\epsilon_{total}) \mathbf{L}^{-1}. \qquad (11)$$

Note that this simplification only leads to a faster PUL computation and does not affect the operation of our proposed solution. We then feed these PUL parameters into the open-source channel generator tool of [26] to obtain CFRs of different aging profiles and under varying load and network topology conditions.

C. Grid Topology

Grid surveillance and diagnostics are conducted by the utility company that already has knowledge of the grid topology. Thus, we consider a static network topology as shown in Fig. 2, where TX and RX indicate the locations of two SG PLMs alternatively operating as a transmitter and a receiver, respectively, BP is a branch point, and BE is an equivalent

branch termination load. Note that the network shown in Fig. 2 is only a part of the operating grid and the impedances seen by the line at the nodes TX, RX, and BE are equivalent aggregated load representations of a possibly more complicated grid topology.

D. CFR Generation

Along with specifying the PUL parameters and the network topology, CFR generation also requires the knowledge of the wire configuration. We consider a symmetric three conductor configuration; specifically, the XLPE multi-core cable N2XSEY from HELUKABEL with equidistant conductor separations of $d_{0,1} = d_{0,2} = d_{1,2} = d_{cond}$ and equal conductor radii $r_0 = r_1 = r_2 = r_{cond}$. All properties of the cable required to compute the PUL parameters are also listed in Table II.

Next, we specify the severity of cable degradation in the form of γ_{homo} and γ_{local}. To determine a realistic limit for γ_{homo} associated with an aging profile, we apply $t = t_{max} = 30$ years in (3), which is the life expectancy of a service-aged cable [3, Ch. 6]. Further, for the computation of F in (3), we consider the electric field at a distance r_{cond} from the center of the conductor, where the electric field strength is at its maximum and is most prone for WT growth initialization [28]. By applying approximate cylindrical geometry as [28, Eq. 1], we get

$$F = \frac{V_0}{r_{cond} \ln\left(\frac{d_{cond}}{2r_{cond}}\right)}. \qquad (12)$$

With (3) and (12), we can thus compute $\max(\gamma_{homo}) = 0.0481$ at $t_{max} = 30$ years. Therefore, we let $0 \leq \gamma_{homo} \leq 0.05$ in our evaluations. In order for a localized WT degradation to be noticeable, we further limit $\gamma_{local} > 0.1$.

Finally, we use the network topology shown in Fig. 2, with the segment lengths of $TX - BP$, $BP - RX$, and $BP - BE$ to be 500 m, 500 m, and 100 m, respectively. Using these values, we generate CFRs with a frequency resolution of 24.414 kHz in accordance with the HomePlug Green PHY and IEEE 1901 Access specifications [29], [30].

IV. GRID SURVEILLANCE METHODOLOGY

In this section, we present the remote grid surveillance and auto-diagnosis procedure that we propose for self-reliant grid diagnostics.

A. Surveillance Procedure

We use the CFR estimated at the PLMs to continuously monitor the status of the line. In the first step, we pass every CFR into a degradation-type classifier to identify whether a
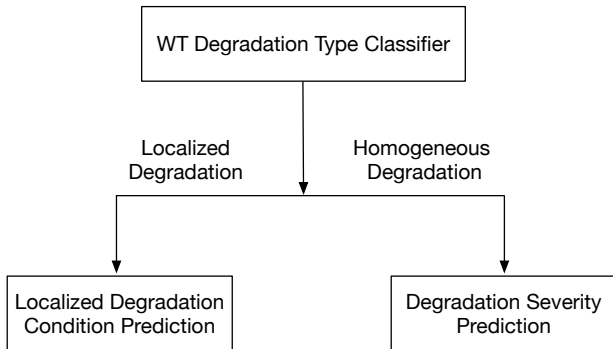
Fig. 3. Proposed road-map for a self-reliant grid surveillance.

Fig. 4. Channel frequency response with homogeneous and localized WT degradations.

localized WT degradation is present on the main line (either between TX−BP or BP−RX). If the localized WT degradation is present on BP − BE, we rely on other PLMs for whom the degradation lies on their main line. If no salient localized WT degradation is identified, we classify them as cables with homogeneous degradation, and predict the degradation severity γ_{homo} along the cable. On the other hand, if a localized WT degradation is identified, we assess its condition by predicting the associated γ_{local} and ℓ_{wt}. We let the PLMs perform all these actions independently by using ML techniques described in Section IV-B.

B. Constructing the Classifier and Predictor

We use ML classifiers for degradation-type classification and ML regressors for the degradation condition prediction. We apply supervised learning techniques where we train our machine with the CFRs generated under different load conditions as well as their known aging profiles. We use the adaptive boosting (AdaBoost) algorithm for classification, which exhibits extraordinary adaptability in iteratively consolidating multiple weak learners into a strong learner without requiring manual tuning of machine parameters [32]. For the same advantages, we also use least-squares boosting (LSBoost) for regression.

The performance of classification and regression relies significantly on the features that are chosen to train the machine. To determine potentially useful features, we generate intact and degraded CFRs for different degradation types, load conditions, and degradation severity. As an anecdotal observation, Fig. 4 shows the CFRs of a cable with homogeneous WT degradation with $\gamma_{\text{homo}} = 0.025$, and localized degradation with $\gamma_{\text{local}} = 0.5$ under a load condition where the impedance connected between each pair of conductors at the nodes TX, RX, and BE are all equal to 50 Ω. It is noticeable that a localized WT degradation causes increased attenuation at higher frequencies. Through comparisons of CFRs of a localized degradation using different combinations of ℓ_{wt} and γ_{local}, we discovered that this trend holds, and the attenuation also increases with γ_{local} and ℓ_{wt}. Therefore, we
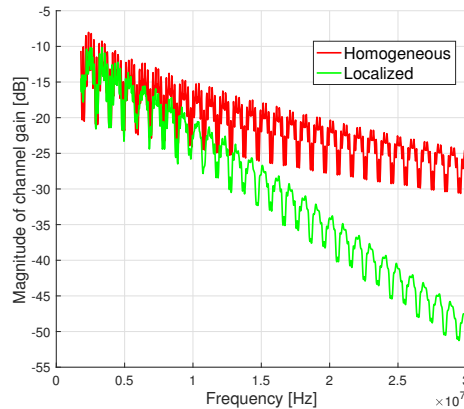
choose the mean and variance of the channel attenuation over all frequency bins in the BB-PLC operating band as two of the features to train our machine. A prior work also suggests that the kurtosis and skewness of the CFR magnitude and phase are helpful in identifying the presence of a localized WT degradation [11]. Thus, we also include these features for our machine training. Further, as the velocity of signal propagation, $v = (\mu \Re(\epsilon_{\text{total}}))^{-\frac{1}{2}}$, is dependent on the relative permittivity, $\Re(\epsilon_{\text{total}})$, of the surrounding medium, the time domain channel impulse response also provides insight into the degradation condition. In particular, we use the peak locations in the channel impulse response as another feature in our machine.

V. SIMULATION RESULTS

Using the PUL parameter computations, CFR generation strategy, and the ML-based grid surveillance techniques proposed in the previous sections, we perform a numerical evaluation of our surveillance methods in MATLAB. For our results, we assume a perfect channel estimate at the PLM receiver as we are currently interested in determining if channel characteristics are actually useful in obtaining meaningful diagnostics results. To generate CFRs under different load conditions, we set the load connected between each pair of conductors at the nodes TX, RX, and BE with a randomized impedance value conforming to $\mathscr{U}(0, 50) + j\mathscr{U}(-50, 50)$ Ω. For homogeneous degradations, we let $\gamma_{\text{homo}} \sim \mathscr{U}(0, 0.05)$, while for localized degradations we select $\ell_{\text{wt}} \sim \mathscr{U}(100, 300)$ m whose centre lies randomly within 100 m from the centre of the cable segment.

A. Degradation-Type Classification

The first step of our surveillance procedure is to detect the presence of a localized degradation. To this end, we compare our results using the AdaBoost algorithm with a classical supervised classification method of support vector machine (SVM), which is also used in [11] for cable diagnostics. We use the linear kernel as well as a radial basis function (RBF) kernel for the SVM. For both types of classification
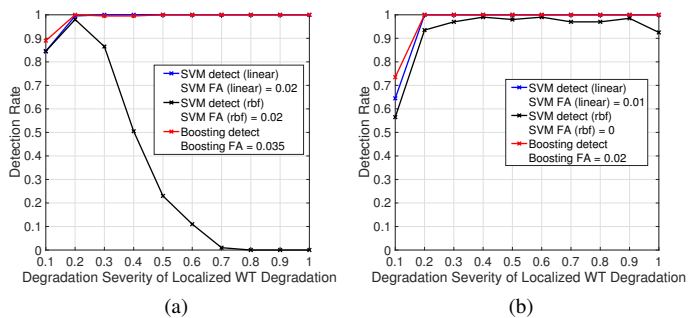
(a)　　　　　　　(b)

Fig. 5. Detection and false alarm rates versus γ_{local} when trained with (a) $\gamma_{\text{local}} \sim \mathscr{U}[0.1, 0.2]$ and (b) $\gamma_{\text{local}} \sim \mathscr{U}[0.1, 1]$

algorithms, we train our machine with 1000 CFRs generated with a homogeneous degradation, and 2000 CFRs with a localized degradation of $\ell_{\text{wt}} = 200$ m located evenly in either the $\text{TX} - \text{BP}$ section or the $\text{BP} - \text{RX}$ section. For testing, we generate 100 samples for each γ_{local} condition, including $\gamma_{\text{local}} = 0$ that denotes the condition without a localized degradation.

The results of detection and false alarm (FA) rates are shown in Fig. 5. Fig. 5(a) presents the rates when the machine is trained with localized degradations of $\gamma_{\text{local}} \sim \mathscr{U}[0.1, 0.2]$. In this case, AdaBoost shows excellent adaptability and performance over an extended range of tested γ_{local}. On the other hand, the performance of SVM strongly depends on the machine parameters tuning, i.e., the kernel function. However, when trained with a wider range of $\gamma_{\text{local}} \sim \mathscr{U}[0.1, 1]$, all methods present similar performance results, as shown in Fig. 5(b). In practical scenarios, we envision the training samples typically to be obtained from manually degraded cables. Therefore, a machine that is able to better learn the cable conditions using a smaller range of training γ_{local}, which in this case is achieved with AdaBoost, could be potentially more beneficial. At the same time, AdaBoost also presents better detection rates and lower FAs in both training scenarios, which justify our proposition of its use.

B. Equivalent Cable Age for Homogeneous Degradation

Once a cable is identified to be free of a localized WT degradation, we use the LSBoost regression algorithm to predict γ_{homo}. We then use this predicted γ_{homo} to calculate the equivalent cable age by rewriting (3) to get

$$t = \sqrt[3]{\left(\frac{Y \cdot y_{\text{homo}}^3}{n_0 v_0 f_0 F^2 \epsilon_0 \Re\{\epsilon_w\}} \right)^2}, \qquad (13)$$

which is the equivalent service age of the considered cable under nominal conditions specified with the parameters listed in Table I. This equivalent cable age provides an intuitive indication of the overall cable degradation extent and its remaining life expectancy.

In this evaluation, we train the regressor with 3600 samples of γ_{homo} varying from 0 to 0.05. We then test with 1000 random CFRs with different load conditions and varying γ_{homo} between 0 to 0.05. The evaluation results are shown in Fig. 6,
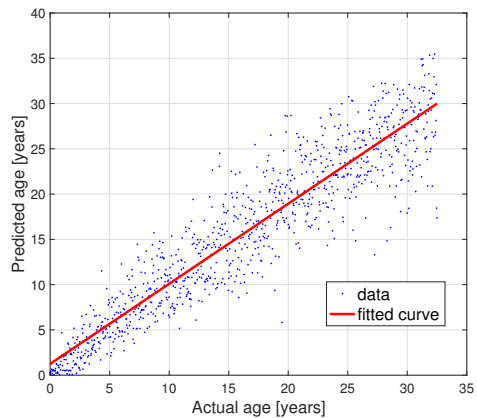

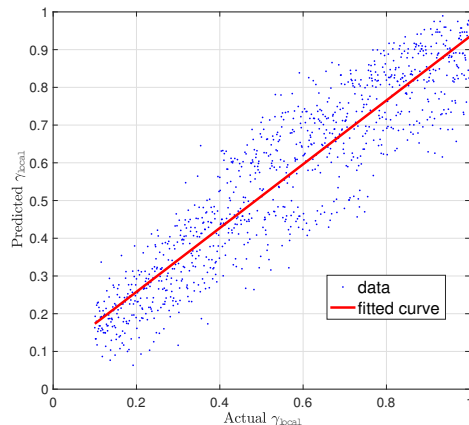Fig. 6. Performance of age prediction for homogeneous cable degradations.

Fig. 7. Predicted γ_{local} versus actual γ_{local} for localized degradations.

where we plot the variation of the predicted t for different actual values of t. We clearly notice that the linear fit of the prediction data has a near unity slope with a negligible ordinate intercept, indicating a successful performance.

C. Predicting the Condition of a Localized Degradation

If a cable is identified with a non-homogeneous degradation, i.e., localized WT degradation, we predict its associated γ_{local} and ℓ_{wt}. In our evaluation, we randomly place the localized degradation in the $\text{TX} - \text{BP}$ or the $\text{BP} - \text{RX}$ branch during both training and testing.

1) Prediction of γ_{local}: We train the regressor with 3600 samples of γ_{local} varying in equal steps from 0.1 to 1, and test with 1000 random CFRs generated with γ_{local} between 0.1 and 1. The performance of our regressor is shown in Fig. 7. We observe that our predicted γ_{local} is around the actual γ_{local} across all values. We also notice a non-negligible variance of the actual data around the linear fit as we train and test with different degradation lengths, degradations locations, and load conditions. However, we note that an accurate value can be obtained by averaging over multiple evaluations.

2) Prediction of ℓ_{wt}: We found through our evaluations that a direct prediction of ℓ_{wt} yields unsatisfactory results. However, significant improvement in performance was observed when we attempted to predict the product $(\gamma_{\text{local}} \cdot \ell_{\text{wt}})$ instead.
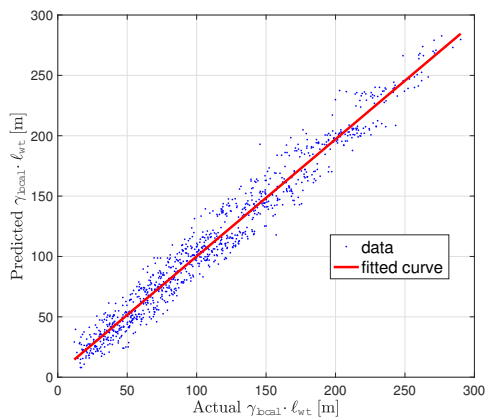
Fig. 8. Predicted $\gamma_{\text{local}} \cdot \ell_{\text{wt}}$ versus actual $\gamma_{\text{local}} \cdot \ell_{\text{wt}}$ for localized degradations.

In this way, we can use the predicted ($\gamma_{\text{local}} \cdot \ell_{\text{wt}}$) together with the predicted γ_{local} to determine ℓ_{wt}. To this end, we employ the same training and testing scenarios as in Section V-C1. The resultant performance is shown in Fig. 8, which reveals that our predicted ($\gamma_{\text{local}} \cdot \ell_{\text{wt}}$) not only closely matches the actual values, but also provides relatively low variance around its linear fit.

VI. Conclusion

In this paper, we have presented solutions to enable power line modems to independently monitor and detect cable degradations using machine learning techniques. We tested our proposed solutions with WT degradations in XLPE cable insulations. To faithfully emulate realistic WT degradations, we devised a scheme to generate CFRs for a given network topology with any considered aging profile along the cable with reduced computation complexity. We then showed through simulation results that our solutions can successfully classify homogeneous and localized WT degradations with an accuracy of over 90% under lower degradation severities, and provide perfect detection rates at more severe degradations. Further, we also successfully predicted the equivalent cable age with homogeneous degradations, and estimated the degradation severity and the length of affected cable region for localized degradations. Our cable aging profile prediction presents the first results of this kind using PLC, which could further be improved by designing methods to localize degradations and evaluate the performance under varied types of faults and degradations.

References

[1] H. Farhangi, "The path of the smart grid," *IEEE Power and Energy Magazine*, vol. 8, no. 1, pp. 18–28, 2010.

[2] S. Fawkes, *Energy efficiency: the definitive guide to the cheapest, cleanest, fastest source of energy*. Routledge, 2016.

[3] P. Gill, *Electrical power equipment maintenance and testing*. CRC press, 2008.

[4] P. Wang, M. R. Raghuveer, W. McDermid, and J. C. Bromley, "A digital technique for the on-line measurement of dissipation factor and capacitance," *IEEE Transactions on Dielectrics and Electrical Insulation*, vol. 8, no. 2, pp. 228–232, 2001.

[5] V. Dubickas, *On-line time domain reflectometry diagnostics of medium voltage XLPE power cables*. PhD thesis, KTH, 2006.

[6] J. Perkel and J. C. Hernandez-Mejia, "Medium voltage cable system partial discharge," http://www.neetrac.gatech.edu/cdfi-publications.html, 2016.

[7] M. Ahmed and W. L. Soo, "Power line carrier (PLC) based communication system for distribution automation system," in *IEEE International Power and Energy Conference*, pp. 1638–1643, 2008.

[8] Itron, "Openway powered by itron riva technology," https://www1.itron.com/Documents/OpenWay-Riva.pdf, 2014.

[9] M. O. Ahmed and L. Lampe, "Power line communications for low-voltage power grid tomography," *IEEE Transactions on Communications*, vol. 61, pp. 5163–5175, December 2013.

[10] F. Passerini and A. M. Tonello, "Analysis of high-frequency impedance measurement techniques for power line network sensing," *IEEE Sensors Journal*, vol. 17, no. 23, pp. 7630–7640, 2017.

[11] L. Förstel and L. Lampe, "Grid diagnostics: Monitoring cable aging using power line transmission," in *IEEE Int. Symp. Power Line Commun. and its Appl. (ISPLC)*, pp. 1–6, 2017.

[12] A. M. Lehmann, K. Raab, F. Gruber, E. Fischer, R. Müller, and J. B. Huber, "A diagnostic method for power line networks by channel estimation of PLC devices," in *IEEE International Conference on Smart Grid Communications (SmartGridComm)*, pp. 320–325, 2016.

[13] J. A. Jiang, C. L. Chuang, Y. C. Wang, C. H. Hung, J. Y. Wang, C. H. Lee, and Y. T. Hsiao, "A hybrid framework for fault detection, classification, and location—part I: Concept, structure, and methodology," *IEEE Transactions on Power Delivery*, vol. 26, no. 3, pp. 1988–1998, 2011.

[14] T. S. Abdelgayed, W. G. Morsi, and T. S. Sidhu, "Fault detection and classification based on co-training of semi-supervised machine learning," *IEEE Transactions on Industrial Electronics*, 2017 (preprint).

[15] H. Orton, "History of underground power cables," *IEEE Electrical Insulation Magazine*, vol. 29, no. 4, pp. 52–57, 2013.

[16] J. Densley, "Ageing mechanisms and diagnostics for power cables - an overview," *IEEE Electrical Insulation Magazine*, vol. 17, no. 1, pp. 14–22, 2001.

[17] I. Radu, M. Acedo, J. C. Filippini, P. Notingher, and F. Ftutos, "The effect of water treeing on the electric field distribution of XLPE," *IEEE Transactions on Dielectrics and Electrical Insulation*, vol. 7, no. 6, pp. 860–868, 2000.

[18] P. Werelius, *Development and application of high voltage dielectric spectroscopy for diagnosis of medium voltage XLPE cables*. PhD thesis, KTH, 2001.

[19] R. Patsch and J. Jung, "Water trees in cables: generation and detection," *IEE Proceedings - Science, Measurement and Technology*, vol. 146, no. 5, pp. 253–259, 1999.

[20] L. Pruitt, "Conventional and cross-linked polyethylene properties," in *Total Knee Arthroplasty*, pp. 353–360, Springer, 2005.

[21] J. P. Crine and J. Jow, "A water treeing model," *IEEE Transactions on Dielectrics and Electrical Insulation*, vol. 12, no. 4, pp. 801–808, 2005.

[22] G. Mugala, *High frequency characteristics of medium voltage XLPE power cables*. PhD thesis, KTH, 2005.

[23] W. V. Titow, *PVC plastics: properties, processing, and applications*. Springer, 2012.

[24] F. Stucki, "Dielectric properties and IV-characteristics of single water trees," in *IEEJ International Workshop on Electrical Insulation*, pp. 7–10, 1993.

[25] F. Versolatto and A. M. Tonello, "An MTL theory approach for the simulation of MIMO power-line communication channels," *IEEE Transactions on Power Delivery*, vol. 26, no. 3, pp. 1710–1717, 2011.

[26] F. Gruber and L. Lampe, "On PLC channel emulation via transmission line theory," in *IEEE International Symposium on Power Line Communications Its Applications (ISPLC)*, pp. 178–183, 2015.

[27] C. R. Paul, *Analysis of multiconductor transmission lines*. John Wiley & Sons, 2008.

[28] W. Shu, J. Guo, and S. A. Boggs, "Water treeing in low voltage cables," *IEEE Electrical Insulation Magazine*, vol. 29, no. 2, pp. 63–68, 2013.

[29] "Homeplug green PHY specification," *HomePlug Powerline Alliance*, 2010.

[30] "IEEE standard for broadband over power line networks: Medium access control and physical layer specifications," *IEEE Std 1901-2010*, pp. 1–1586, 2010.

[31] HELUKABEL, "Medium voltage power cables," http://mdmetric.com/prod/helukabel/N.Medium%20Voltage%20Power.pdf, 2016.

[32] Y. Freund and R. Schapire, "A short introduction to boosting," *Japanese Society For Artificial Intelligence*, vol. 14, no. 5, pp. 771–780, 1999.